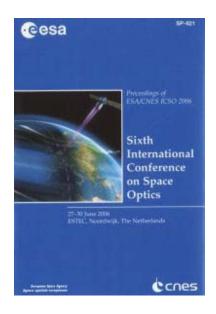# International Conference on Space Optics—ICSO 2006

Noordwijk, Netherlands

27–30 June 2006

Edited by Errico Armandillo, Josiane Costeraste, and Nikos Karafolas

Demonstrator study for micro-ranging-laser device

Hartmut Henkel, Bodo Bernhardt, J. Pereira do Carmo

DEMONSTRATOR STUDY FOR MICRO-RANGING-LASER DEVICE

Hartmut Henkel[1], Bodo Bernhardt[1], and J. Pereira do Carmo[2]

[1]von Hoerner & Sulger GmbH, D-68723 Schwetzingen, Germany; Email: henkel@vh-s.de, bernhardt@vh-s.de
[2]ESTEC TEC-MMO, 2200 AG Noordwijk ZH, The Netherlands; Email: joao.pereira.do.carmo@esa.int

ABSTRACT

Within ESA's Innovation Triangle Initiative (ITI) a demonstrator breadboard for a micro-ranging-laser device "MYL-RAD" has been developed. Its working principle is the measurement of the round-trip delay time of a laser beam as a phase shift. The demonstrator consists of the laser diode (30 mW, square wave AM), optics, APD detector, narrowband preamplifier, limiter, and a phase digitiser based on a novel noise-shaping synchroniser (NSS) circuit; this works without ADCs and can be built from rad-hard components for space. The system timing and the digitiser algorithm are performed by an FPGA. The demonstrator has been tested at ranges from 1 m to 30 m. With a static non-cooperative target an RMS noise of 1 mm at a result rate of 60 Hz was reached. The demonstrator needs less than 2.5 W power.

Key words: LIDAR, Laser Radar, 3-D Scanner.

1. INTRODUCTION

1.1. LIDAR Applications in Space

LIDAR (Light Detection and Ranging) systems derive the distance (range) $s = tv_0/2$ between them and a target object by measuring the round-trip travel time t of a signal carried by a laser beam at speed of light v_0 and reflected at the target (e. g. a distance of 1 m corresponds to a delay of ≈ 6.67 ns). The LIDAR principle has a very high precision, as it uses the fundamental constant v_0, and there are various methods known for precise measurement of t.

LIDAR systems have broad applications in space for navigation, guidance, and exploration; a few examples are given in the following: Docking manoeuvres between satellites require precise real-time knowledge of the relative position between them. Establishing satellite formations and clusters for looking into deep space with an extended geometrical baseline requires very precise position control between the formation members; when highest distance accuracy is required, complex systems based on light interferometry outperform LIDAR, but they often still use a LIDAR for coarse range measurement. In laser altimetry the geometrical form of a planetary body can be measured by a LIDAR on-board of an orbiting spacecraft, which is a scanning system by principle due to orbiter. Another LIDAR application are descent manoeuvres for landing on planetary or cometary bodies. For planetary exploration, after landing, LIDAR systems in combination with a scanning device (e. g. moving mirror) can be used for acquiring 3-D volume images of the space surrounding a lander or robotic vehicle. Volume images by scanning LIDAR have several advantages over 3-D images from stereo cameras: The 3-D volume image information from a LIDAR arrives point by point already during acquisition, whereas stereo camera based systems require heavy image processing for calculation of the volume image from textural image information. Both 3-D imaging methods can also beneficially complementing each other.

For all above application there are often strict limitations in mass, volume and power budget. Also these LIDAR systems should have very high reliability.

1.2. Outline of the Presented Activity

Within ESA's Innovation Triangle Initiative (ITI), a demonstrator breadboard for a miniaturised LIDAR system has been developed, built, and its performance has been tested. The activity was performed in 2005. This breadboard has been named "Micro-Ranging-Laser Device", for short "MYLRAD". Two aspects led to this project: First, the interest in miniaturised LIDAR systems has been apparent to the authors due to their activity in the area of planetary exploration and robotic devices. Second, a method and apparatus for digitisation of phase shifts had already been developed and patented (1) by one of the authors. The great potential of this method for precise time delay measurement in the context of a LIDAR application had been identified. The "MYLRAD" breadboard is a first proof-of-concept for this method.

1.3. LIDAR Principles

LIDAR systems require modulated laser light for operation. There are two main modulation methods: short-pulse and continuous modulation. For both methods we give here a brief overview. LIDARs with short-pulse modulation perform a range measurement by emitting a short (typ. < 2 ns, depending on range resolution) laser light impulse. The time between the emitted and the received laser pulse is measured (2; 3), Patents (4; 5; 6; 7). LIDARs with continuous modulation instead emit laser light that is periodically amplitude modulated (other modulation schemes are possible). Here the delay time appears as a phase shift between the emitted and the received laser light modulation. In both cases the transmitted laser pulse can be collimated, and the light reflected by the target is acquired by a receiver optics with opto-electrical converter (e. g. Avalanche photodiode, APD).

There are notable differences between LIDAR systems using pulsed vs. continuous modulation regarding hardware implementation as well as operation: One main limiting factor for the range resolution of short-pulse LIDARs is the minimum duration of the laser pulse. For high range resolution, laser pulses with duration in the order of nanoseconds or below are required. For high photonic throughput with these short pulses one needs high instantaneous laser power. This can often be provided only by a solid-state laser that is pumped e. g. by laser diodes (single, or arranged as bars or stacks). Due to the two-stage light generation in these systems and the requirement of an active or passive q-switch within the solid-state laser they generally have a rather high hardware complexity. One important application for pulsed LIDARs stems from the fact, that the short laser pulse reflected by semi-transparent layers like clouds can also be acquired, so that the received light might be a stretched version of the transmitted pulse, carrying information about the volume reflectivity. Due to the generally short duration of the received light pulse the opto-electrical detector and the analog frontend must have a rather high bandwidth and phase linearity.

In comparison, LIDARs with continuous modulation can work with a single laser diode that is quasi-continuously (QCW) amplitude modulated, e. g. by a square wave with duty cycle of 50 %. Here the laser output power has a much lower peak factor than the pulsed laser as described above, so that this modulation scheme utilises the continuous power handling capability of the laser diode much better, and with a lower current stress to the laser diode (which contributes to increased reliability). This allows to use laser diode based LIDAR systems (no solid-state laser) for applications up to a few kilometers. Due to the continuous modulation of the laser carrier, and due to the fact that the distance is contained in the phase shift of the received periodic signal, the receiver frontend amplifier can be a narrow-band design, which requires less power than the wide-band design of a receiver for a pulsed system.
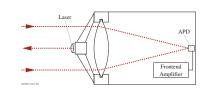

Figure 1. Coaxial arrangement of laser emitter and receiver.

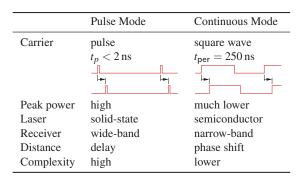|	Pulse Mode	Continuous Mode
Carrier	pulse $t_p < 2$ ns	square wave $t_{per} = 250$ ns
Peak power	high	much lower
Laser	solid-state	semiconductor
Receiver	wide-band	narrow-band
Distance	delay	phase shift
Complexity	high	lower

Table 1. Comparison of LIDAR modes.

Another difference between the described methods is in the handling of stray light propagating from the transmitter side into the receiver optics. This can be a critical factor, as the transmitted laser energy is several orders of magnitude higher than the faint light energy received from a far target. With a pulsed system the near echoes can be blanked out by a gating circuit inside the receiver, as the light has completely left the transmitter when the echo is received. This is not possible with the QCW modulated system; the transmitter is still sending out light while reflected light is already received. This cross-coupling is an important issue of the QCW LIDAR systems, but it can be alleviated by proper positioning of the laser diode relative to the receiver optics, e. g. as shown in Fig. 1.

A comparison of the discussed main differences is summarised in Table. 1. Due to their low complexity, QCW LIDAR systems using only laser diodes are better suited for miniaturisation than pulsed systems. As our interest is primarily in a technically simple and robust, miniaturised LIDAR system for opaque targets only, and with applicability in near range (0 m. . . 30 m, but extendable) we chose the promising QCW LIDAR method with a low-power laser diode for the MYLRAD breadboard.

2. THE MYLRAD BREADBOARD

The block diagram of the MYLRAD demonstrator breadboard is shown in Fig. 2. In the top part is the transmitter system: A quartz stabilised clock generator circuit (frequency 80 MHz) provides the master clock for the overall MYLRAD system. The clock is divided down to a frequency of 4 MHz providing the modulation signal (carrier) for the laser diode. This signal is fed into a laser diode
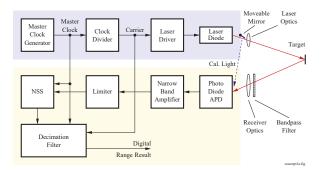
Figure 2. Block diagram of the MYLRAD breadboard.

Figure 3. Principle of phase measurement by analog integrator.

driver circuit, where the laser diode current is controlled and amplitude modulated with a duty cycle of 50 %. The outgoing laser beam is collimated by a miniature optics that is part of the laser diode assembly. The lower part of the block diagram shows the receiver signal chain of MYLRAD, starting with a receiver optics lens of diameter 22 mm. In the focus of this lens an Avalanche photodiode (APD) as opto-electric converter is positioned. The APD is supplied by a voltage in the order of 100 V, providing a conversion gain of ≈ 100. The electrical output signal from the APD is amplified by a integrated low-noise narrow band amplifier, containing LC and quartz filters. The amplifier output is fed into a limiter circuit which must be capable of handling input signals with very large dynamic range due to the multiplicative effect of varying range and reflectivity of the targets. The limiter converts this analog echo signal into a purely digital one with logic levels '0' and '1'. The range information is then contained in the analog-time positions of the edges of this digital signal; any amplitude information is thereby discarded. The range information can now be derived by measurement of the continuous phase shift between the carrier signal used for laser modulation and the digital limiter output signal. Within MYLRAD this phase shift is digitised by a circuit consisting of a novel "noise-shaping synchroniser" ("NSS") and a digital decimation filter, as described below.

2.1. General Delay Measurement

Measurement of the delay between the signal modulated onto the transmitted laser beam and the digital echo signal derived from the light reflected by the target requires a method for precise measurement of phase shifts. There exist several circuit concepts for achieving this. E. g., one can use a high-frequent clock for establishing a time base and count the clocks between transmitted and received signal. The varying range is represented by the sequence of count values for each echo. This method has the drawback that it requires a very high clock frequency if a high range resolution is required (e. g., 15 GHz clock frequency for 1 cm range resolution). Another method uses an analog integrator, where a voltage is linearly increasing with a known rate, and synchronously with the modulation of the
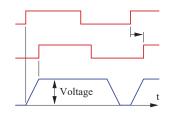
transmitted laser beam. This ramping voltage can then be sampled when the echo is received; this is illustrated by Fig. 3. The sampled voltage value, which represents the phase shift, can be digitised by an analog/digital-converter (ADC). This principle has the advantage that it has a very high time resolution due to the analog nature of the sampled ramping voltage. However, as the range is contained in an analog voltage, the high resolution is limited in practice by analog drift effects and the performance of the ADC. The MYLRAD breadboard instead uses a novel method for phase measurement that combines the advantages of the both above described methods, while avoiding their drawbacks.

2.2. The Noise-Shaping Synchroniser

As shown in Fig. 2, the echo signal from the limiter output enters a building block "Noise-Shaping Synchroniser" ("NSS"). The purpose of this circuit is to synchronise the received echo signal onto the 80 MHz clock from the master clock generator. Here the complication is that this should happen without losing time resolution, and without the need for a master clock in the order of several GHz—which seem to be contradictory requirements at the first glance. Once the echo signal is in the digital clock raster, it can be further processed by digital algorithms, providing in the final range output. A simple sampling of the digital echo signal onto the master clock by means of a flip-flop would add a significant time quantisation error, as the exact analog-time positions of the echo signal edges between two master clock edges would be ignored and lost. A circuit is required that preserves the analog fine timing between two master clock edges. Else one would need a very high master clock as described above for the counter method.

The solution for this problem can be found by adapting concepts "noise shaping", "oversampling", and "decimation filtering" (8) that are in wide use e. g. in modern Delta-Sigma ($\Delta\Sigma$) ADCs, as outlined in the following: For the LIDAR phase measurement one can profit from the point, that the range information is normally required only with a much lower sampling rate (e. g. 1 kHz) than the modulation frequency (here 4 MHz) of the laser. This means that to get one digital range result one can process a sequence of several thousand echoes. The "NSS" performs the synchronisation of the limiter output signal—
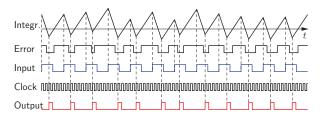
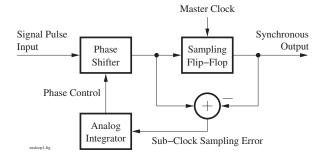*Figure 4. Signals at the noise-shaping synchroniser.*

Figure 5. Principle diagram of the 1st order noise-shaping synchroniser.

which contains the range in the analog-time position of its edges—on the clock raster in a particular "noise-shaping" way. The resulting digital pulse stream output from the NSS has three properties that are depicted in Fig. 4: First, every input impulse results in one output impulse. Second, the output pulse stream is strictly in the digital time raster of the 80 MHz master clock (the individual pulse edges do not coincide with the analog-time edges of the echo signal any more), so the pulse stream can be further processed by purely digital algorithms, e. g. in an FPGA or ASIC. Third, the digital pulse stream output of the NSS still contains the precise analog edge positions of the original echo signal in the *average* of many pulse positions. By calculating the average phase shift of the digital pulse stream output from the NSS one can derive the phase shift of the analog echo signal, and therefore the range of the target, with high precision.

The functional principle of the NSS is illustrated by Fig. 5. The input echo signal is fed into an analog phase shifter and is then sampled to the master clock by a flip-flop. The sampling process introduces a time quantisation error, as mentioned above. But this error is not lost; instead it is accumulated as analog voltage in a high-speed integrator circuit, which in turn controls the analog phase shifter. By this feedback loop the accumulated quantisation error is recursively taken into account when sampling the next echo signal edge by pre-compensation of the incoming echo signal edge position. The resulting synchronous pulse stream appears to be "dancing around" the correct analog-time echo in a well-defined way, and with a fixed and known time offset.

The spectral "noise-shaping" effect of the NSS can be seen if one builds an FFT of the sequence of phase shifts
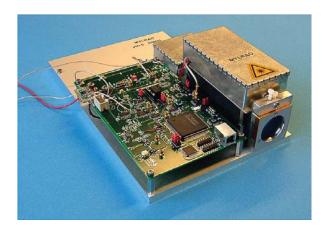

Figure 6. Photo of the MYLRAD breadboard.

from the digital output pulse stream: The seemingly incorrect positions of the NSS output pulses (see Fig. 4) have the property in the frequency domain of phases, that the phase error introduced by the NSS synchronisation (= time quantisation) is shifted away from the base band towards higher frequencies. But only the base band contains the relevant original range information. By digital low-pass filtering of the sequence of echo phases using a digital decimation filter the high-frequent phase quantisation noise can be removed, resulting in a new sequence of echo phases that come with the nominal result rate (e. g. 1 kHz), but then with strongly reduced quantisation noise. This corresponds to an increased range resolution—much larger than the phase raster given by the master clock; the decimation filter delivers multi-bit words at the result rate.

As a summary, the phase digitisation of LIDAR echoes within the MYLRAD system is done in two steps: First the edge positions of echoes from the limiter output are synchronised to the master clock raster by the NSS, whereby time quantisation takes place, then the resulting sequence is lowpass-filtered by a digital decimation filter, resulting in the digital range information with high resolution. No ADC is needed for this process at all. By programming only the decimation factor of the digital decimation filter the range result rate can be traded in for phase quantisation noise: If a higher result rate is needed, the range precision will be lower, whereas a lower result rate results in high range precision. No changes in the NSS parameters are required. Finally, one can compare the NSS concept with the ones of widely known ΔΣ voltage ADCs: These ADCs perform noise shaping to the processed signal voltages, whereas the NSS is an implementation where the noise shaping happens to the processed signal phases.

3. BREADBOARD IMPLEMENTATION

At the begin of the design phase extensive simulations of critical MYLRAD breadboard units have been performed: The NSS algorithm and its circuitry as well as the dig-
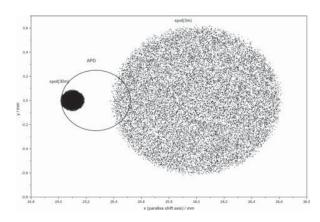
Figure 7. Monte-Carlo simulation of defocussing at the APD plane.

ital decimation filter have been studied by algorithmic simulations programmed in the 'C' and 'calc' languages as well as in Spice. The complete optical path—from the laser diode towards a far non-cooperative target and back onto the active surface of the APD—has been studied by 3-D Monte-Carlo simulations written in 'C'. This allowed to optimise the positioning of the APD at the internal lens focus; the system was focussed at infinity. Here one can profit from the fact, that a target—depending on its distance—produces a more or less defocussed and parallax-offset light spot at the APD, which has an active diameter of 0.5 mm. One such simulation run is shown in Fig. 7. This blurring and parallax effect allows to compensate for part of the intensity variation induced by the large covered target range. Very near targets (< 0.5 m) due to large parallax produce a light spot in the APD plane that does not hit the active APD area at all. This can be alleviated by a small semi-transparent diffuser near the APD; only the light from very near targets hits this diffuser.

After all simulations were performed, the actual hardware- and software design phase followed. The Fig. 6 shows a photo of the ready MYLRAD breadboard, which implements all building blocks from Fig. 2: The laser diode with its driver circuit are in the long shielding enclosure at the top right; the collimated laser beam goes in "southeast" direction. The long optical shielding box below the laser circuit enclosure has the receiver entrance aperture with round lens; the APD is mounted at the end of this box. The square shielding compartment in the middle top contains the APD preamplifier. Great care is taken to shield the receiver against electromagnetic interferences (RF and light) from the transmitter side, which would result in nonlinearities and range locking effects. The NSS and all digital processing circuitry are combined on the Euro-sized PCB that makes up the left side of the MYLRAD breadboard. The digital decimation filter and the overall control are designed in the language Verilog and implemented in a Xilinx Spartan II FPGA. The decimated raw range results are transferred via an USB interface (at the front, next to the receiver lens) to a PC, where the range recording and analysis are done.
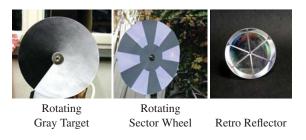

| Rotating Gray Target | Rotating Sector Wheel | Retro Reflector |

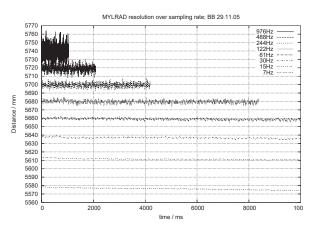*Figure 8. Various range test targets.*

Figure 9. Static range noise with non-cooperative target as function of the result data rate; target at 3 m distance.

4. TESTING OF THE BREADBOARD

The performance of the MYLRAD breadboard has been extensively tested, using various test targets that fall into groups cooperative vs. non-cooperative and static vs. dynamic. Three target examples are shown in Fig. 8. In addition to these tests also tests regarding drift effects over time and temperature as well as tests regarding the influence of ambient light have been performed.

Static cooperative targets present the optimum situation for the MYLRAD: They don't move, and they have a high reflectivity, directing received light back into the receiver optics. An example is the retro reflector prism shown at the right side of Fig. 8. In comparison non-cooperative targets are given by any surface with non-directed reflectivity (e. g. soil or rock). Static targets have a fixed position relative to the MYLRAD, whereas dynamic targets exhibit a relative movement, changing their distance or reflectivity over time. Examples used for testing are the two rotating discs shown in the left and middle of Fig. 8.

Range measurement tests have been performed with these targets over distances between 0.5 m and 30 m. The static range noise for a target at 3 m distance is shown in Fig. 9 as function of the selected result data rate (decimation filter setting); the plotted lines are repositioned vertically to separate them.

Parameter	Value	Comment
Laser power	15 mW	average
Modulation	4 MHz	
Meas. rate	1000 results/s	up to 20 k results/s
Meas. range	0.5 m – 30 m	non-cooperative targets
Extended range	0.5 m – 7 km	cooper. targets, extrapol.
Static range resol.	5 mm – 30 mm	over 0.5 m – 30 m range
Beam divergence	0.7 mrad	depending on collimator
Power consumpt.	< 2.5 W	breadboard, 30 mW laser

Table 2. Specifications of the MYLRAD breadboard.

4.1. Discussion of Tests

The MYLRAD breadboard performed well with static targets. An RMS noise in the order of 1 mm could be achieved with non-cooperative targets at a result sampling rate of 60 Hz, as shown in Fig. 9. Also visible is the overall range drift over time, which was about 1 mm every 8 s under the ambient thermal conditions of the laboratory. The noise performance of MYLRAD was not equally good with dynamic targets. Any moving targets, even ones with visually homogeneous reflectivity, produce an amplitude modulation in the reflected light which in principle should not matter due to the limiter stage. But in the current implementation any amplitude modulation gives a cross-talk into the received echo phase, resulting in an increased range noise. Currently dynamic targets generally produce a range noise of about 20 cm. The opinion is that these effects are introduced by nonlinearities in the analog receiver frontend, and to a lesser degree by laser speckle effects; both are not fundamental particular shortcomings of the applied range measurement principle using amplitude modulation or the precision phase digitisation employed. A summary of the specifications reached with the MYLRAD breadboard are listed in Fig. 2.

5. FUTURE IMPROVEMENTS AND EXTENSIONS

The main purposes of the MYLRAD breadboard study were to investigate 1. a LIDAR method based on a QCW semiconductor laser and 2. the novel NSS method for phase digitisation. Apart from the basic functional LIDAR blocks really needed for testing no other functionality could be implemented within the work frame of the study. E. g., the breadboard system currently does not contain any means for compensation of drift effects. Particularly there is no calibration or zeroing mechanism implemented; but Fig. 2 shows that this can be done e. g. by use of a moveable mirror inside the ranging device that directs a tiny part of the transmitted laser light directly back towards the APD receiver, thereby providing a defined temporary near echo. This is left for a future activity. Also due to the laser modulation frequency of 4 MHz there is an intrinsic range ambiguity with a period of 37.5 m. This does not matter if a target is otherwise known to be within a range slot, e. g. within 0 m and 37.5 m. The phase measurement gives similar high precision also if a target is in another range slot, e. g. between 375 m and 412.5 m. The range ambiguity can in principle be resolved by an additional phase modulation on the transmitter side using a subcarrier with a longer period, e. g. modulation by a pseudo-noise (PN) sequence. On the receiver side this phase modulation can be detected by a correlator which allows to detect in which range slot the target is located. It is likely that the PN sequence generator and phase correlator can be implemented in the existing FPGA. Once the range noise effects with dynamic targets are understood and the MYLRAD system is improved, a future step would be the implementation of a miniaturised scanning device, to acquire true 3-D range images.

6. CONCLUSION

The MYLRAD breadboard developed under ESA's ITI programme is an important proof-of-concept for a miniaturised low-power ranging device employing excitation by a low-power QCW operated laser diode, and exploring a novel noise-shaping algorithm and circuitry for digital precision phase measurement. The range result rate, which is tunable, opens the future possibility to use such a ranging device in conjunction with a scanning mirror for 3-D range imaging without the need of a stereoscopic camera. Current shortcomings of the MYLRAD system regarding the range measurement at dynamic targets have been identified during the testing phase. Curing these known dynamic noise effects will require further detailed analysis and modification of the receiver frontend. The hope is that there will be a possibility to track down these points and to improve the MYLRAD breadboard further during a future development. There are various potential space applications that might benefit from miniaturised LIDAR systems based on the MYLRAD principle.

REFERENCES

[1] German Patent No. 19808874, Verfahren zur zeitlichen Quantisierung von Binärsignalen.

[2] Dwayne C. Carmer, Lauren M Peterson, Laser Radar in Robotics, in: Proceedings of the IEEE, Vol. 84, No. 2, February 1996, pp. 299–320.

[3] J. M. Vaughan, K. O. Steinvall, C. Werner, P. H. Flamant: Coherent laser radar in Europe, in: Proceedings of the IEEE, Vol. 84, Issue 2, pp. 205–226.

[4] EP 0 738 899: Vorrichtung zur Distanzmessung.

[5] US 5,815,251, US 5,949,531, US 6,336,277, US 6,463,393.

[6] EP 0 932 835: Vorrichtung zur Kalibrierung von Entfernungsmessgeräten.

[7] DE 3540157: Verfahren und Vorrichtung zur Entfernungsmessung.

[8] James C. Candy, Gabor C. Temes: Oversampling Delta-Sigma Data Converters, IEEE Press, 1992.